

Communication

5-Fluorouracil/Coumarin and 5-Fluorouracil/Chromone Hybrids: Synthesis and Drug-Likeness Modeling

Laura Giraldo-Arroyave, Andrés F. Yepes and Wilson Cardona-Galeano * 

Chemistry of Colombian Plants Group, Institute of Chemistry, Faculty of Exact and Natural Sciences, Universidad de Antioquia, UdeA, Calle 70 No. 52-21, A.A 1226, Medellín 050010, Colombia; laura.giraldoa@udea.edu.co (L.G.-A.); andresf.yepes@udea.edu.co (A.F.Y.)

* Correspondence: wilson.cardona1@udea.edu.co

Abstract: A series of 5-fluorouracil/coumarin and 5-fluorouracil/chromone hybrids were synthesized with good yields using click chemistry as the key step. The structures of these compounds and all intermediates were elucidated by spectroscopic analysis. Furthermore, pharmacokinetic and drug-like computations taken together indicated that the novel hybrids have a strong possibility to advance to further biological studies.

Keywords: 5-FU; coumarin; chromone; hybrid compounds; click chemistry; drug-likeness modeling

1. Introduction

Coumarins and chromones are widely distributed in nature. Herbal-based beverages containing high levels of these compounds have been used since ancient times in traditional medicine. Coumarins and chromones also are well known because of their diversity of pharmacological properties [1–4], including anti-cancer activity [5–8], particularly in colorectal cancer (CRC) [9–12]. CRC, which makes up 10% of all cancer cases, is the second most common and deadliest kind of cancer worldwide [13]. 5-fluorouracil (5-FU) is the basis of the clinically utilized treatment for CRC; while effective, it has a high rate of toxicity and poor tumor selectivity [14]. Consequently, it has undergone modifications to produce conjugates and hybrid compounds, potentially increasing its therapeutic index and lowering its adverse effects [15].

Accordingly, there is an urgent need for new therapeutic molecules and/or approaches to treat CRC. In this regard, molecular hybridization is a promising strategy that has emerged in medicinal chemistry in the search for new therapeutic alternatives. Hybrid molecules bear two distinct pharmacophores with different biological functions [16–19]. In this context, the CuI-mediated Huisgen 1,3-dipolar cycloaddition of azides with terminal alkynes to make 1,2,3-triazoles is a synthetic approach that has been used to create a variety of pharmaceutical agents, including hybrid compounds and drug discovery [20–25]. Using a triazole ring and alkyl chains as linkers, we designed and synthesized a variety of 5-FU-Coumarin and 5-FU-Chromone hybrids in the hunt for novel therapeutic alternatives to treat colorectal cancer (Figure 1). Additionally, pharmacokinetic modeling research was carried out to explore the synthesized hybrids' potential as drug-like compounds.



Citation: Giraldo-Arroyave, L.; Yepes, A.F.; Cardona-Galeano, W.

5-Fluorouracil/Coumarin and 5-Fluorouracil/Chromone Hybrids: Synthesis and Drug-Likeness Modeling. *Molbank* **2024**, 2024, M1779. <https://doi.org/10.3390/M1779>

Received: 6 February 2024

Revised: 23 February 2024

Accepted: 26 February 2024

Published: 28 February 2024



Copyright: © 2024 by the authors. Licensee MDPI, Basel, Switzerland. This article is an open access article distributed under the terms and conditions of the Creative Commons Attribution (CC BY) license (<https://creativecommons.org/licenses/by/4.0/>).

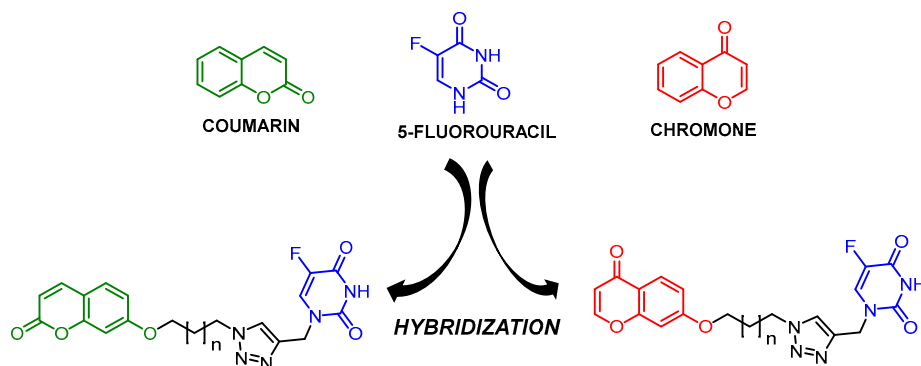
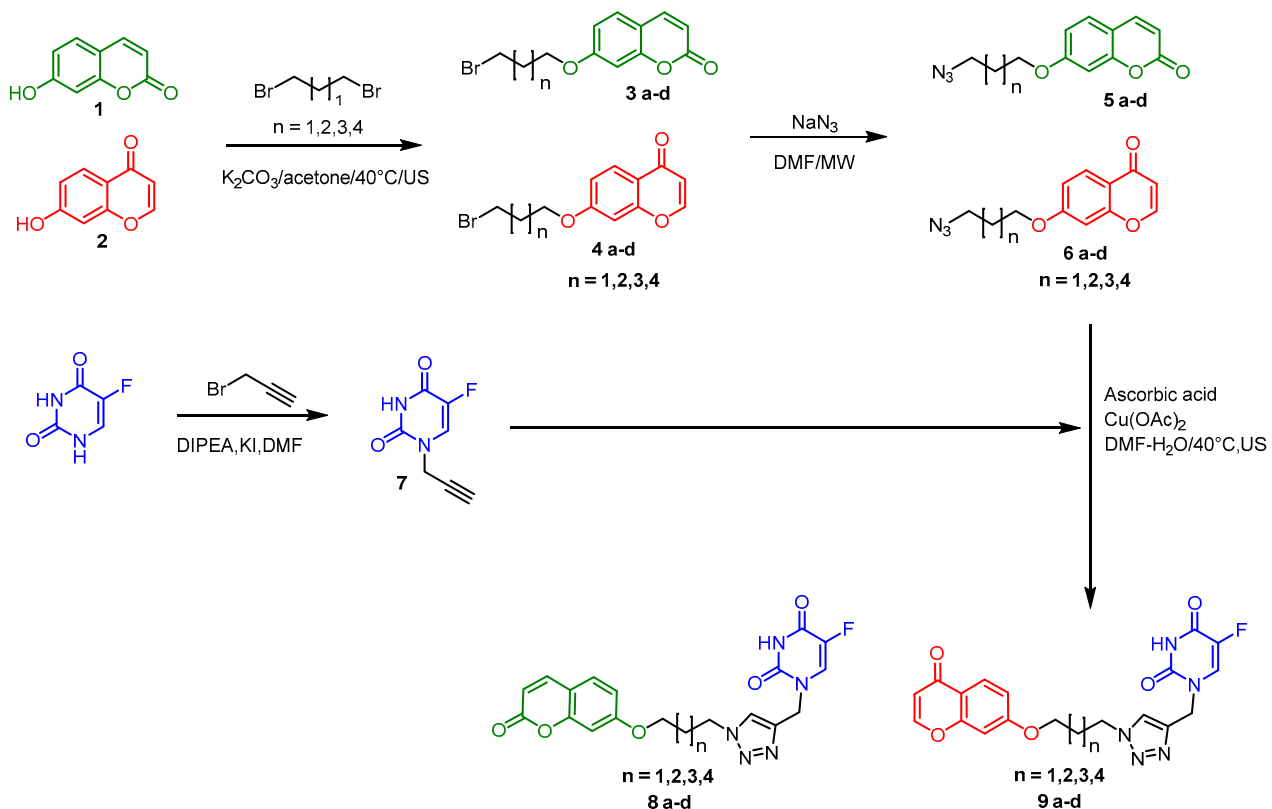


Figure 1. Design of 5-FU-Coumarin and 5-FU-Chromone hybrids.

2. Results and Discussion

2.1. Chemistry

The synthesis of the hybrids began with the obtention of coumarin-bromoalkyl **3a-d** and chromone-bromoalkyl **4a-d** by means of the Williamson ether synthesis of 7-hydroxycoumarin (**1**) and 7-hydroxychromone (**2**) with $1,\omega$ -dibromoalkanes ($\omega = 3, 4, 5, 6$), with yields ranging between 66 and 71% for **3a-d** and 70 and 76% for **4a-d** [26,27]. Compounds **3a-d** and **4a-d** were treated with sodium azide, leading to the formation of the coumarin-alkyl azides **5a-d** (64–70% yields) and chromone-alkyl azides **6a-d** in 67–72% yields [28,29]. Similarly, the reaction of 5-FU with propargyl bromide led to propargyl-5-FU (**7**) with a 40% yield [30]. Finally, the click reaction between compounds **5a-d** and **6a-d** with the alkyne **7** led to the formation of hybrids **8a-d** and **9a-d** with 71–96% and 70–92% yields, respectively [28,31] (Scheme 1). The structures of all compounds were established by a combined study of ESI-MS, ^1H NMR, and ^{13}C NMR.



Scheme 1. Synthesis of hybrids based on 5-FU, coumarin, and chromone.

2.2. Theoretical Pharmacokinetic and Drug-Likeness Studies for Hybrids 8a–d and 9a–d

Biopharmaceutical parameters and drug-like properties for a promising drug candidate play important roles in every stage during the drug development process; in fact, a rule-based filter of drug-likeness could be used for distinguishing an attractive and safer new bioactive molecule in all therapeutic areas. In this section, for hybrids 8–9(a–d), we carried out early predictions of the twelve biopharmaceutical parameters that most significantly impact a molecule's drug-like characteristics, which are as follows: molecular mass (MW), number of H-bond donors/acceptors, number of rotatable bonds, topological polar surface area (TPSA), partition coefficient (as log P_{o/w}), Caco-2 and MDCK permeability values, and human serum albumin (HSA) binding (as logK_{HSA}), the fraction of sp³ carbon atoms, and the number of aromatic/heteroaromatic rings. In addition, the pan-assay interference compounds (PAINS) filter, which is frequently a serious alert in contemporary drug discovery, was applied for compounds 8–9(a–d). Table 1 shows the drug-likeness and pharmacokinetic profile predictions provided by the application of the SwissADME program for 8–9(a–d).

Table 1. Computed biopharmaceutical and drug-likeness indices for hybrids 8–9(a–d).

Properties	Hybrid							
	8a	8b	8c	8d	9a	9b	9c	9d
MW ^a	413.364	427.391	441.418	455.44	413.364	427.391	441.418	455.44
TPSA ^b	125.01	125.01	125.01	125.01	125.01	125.01	125.01	125.01
n-RB ^c	7	8	9	10	7	8	9	10
n-ON ^d	8	8	8	8	8	8	8	8
n-OHNH ^e	1	1	1	1	1	1	1	1
log P _{o/w} ^f	1.31	1.70	2.09	2.48	1.31	1.70	2.09	2.48
logK _{HSA} ^g	-0.314	-0.216	-0.231	-0.034	-0.314	-0.216	-0.231	-0.034
Fsp ³ ^h	0.21	0.25	0.29	0.32	0.21	0.25	0.29	0.32
#ArRNG ⁱ	3	3	3	3	3	3	3	3
Caco-2 ^j	141	111	94	115	141	111	94	115
App. ^k	106	81	46	84	106	81	46	84
MDCK ^k	106	81	46	84	106	81	46	84
PAINS ^l	0	0	0	0	0	0	0	0

^a Molecular weight of the compound (150–500). ^b Polar surface area (PSA, Å²) (<140 Å²). ^c Number of rotatable bonds (optimal: <10). ^d n-ON number of hydrogen bond acceptors <10. ^e n-OHNH number of hydrogens bond donors ≤5. ^f Octanol–water partition coefficient (-2.0 to 6.5). ^g Binding serum albumin (-1.5 to 1.2). ^h Fraction of sp³ carbon atoms (optimal: Fsp³ < 0.5). ⁱ The number of aromatic/heteroaromatic rings (optimal: ≤ 3). ^j Human intestinal permeation, nm/s (<25 is poor, >500 is great). ^k Madin-Darby canine kidney (MDCK) cell permeation, nm/s (<25 is poor, >500 is great). ^l Identification of potentially problematic fragments for pan-assay interference compounds (PAINS).

In general, optimal pharmacokinetic parameters were found for hybrids 8–9(a–d) compared to major of oral FDA-approved drugs. An advantageous level of lipophilicity (represented as logP_{o/w}) was calculated for 8–9(a–d), which falls well inside the ideal range (-2.0 to 6.0) for formulations based on orally administered drugs [32]. Additionally, hybrids 8–9(a–d) had a good predicted permeability index of approximately 141 to approximately 94 nm/s when conventional Caco-2 and MDCK cell models were used, respectively [33–35], indicating that these compounds may have a better chance of being absorbed throughout the intestinal segments when taken orally. The total polar surface area (TPSA), another extremely useful metric that is frequently acknowledged as a good indicator in permeating cell membranes [36], was also computed. The compounds exhibited a TPSA value of 125.01 Å², which is deemed to be a favorable indicator of strong intestinal penetration and falls within the optimal range of less than 140 Å². Additionally, the most important metric for the distribution and transport of drugs and drug candidates in systemic circulation was also predicted for the hybrids: the binding capacity of human serum albumin (measured as logK_{HSA}). Potential medications should have logK_{HSA} values between -1.5 and 1.5, according to ther-

apeutic recommendations [37,38]. The compounds had favorable $\log K_{HSA}$ numbers in the range of -0.034 to -0.314 , which is within the advantageous therapeutic range.

We also investigated both the fraction of carbon atoms that were sp^3 -hybridized (Fsp^3) and the aromatic ring count (#ArRNG), which are two key new drug-likeness parameters relating to the possibility of lability or movement of a molecule through a biological barrier [39–43]. Major commercially available drugs have an Fsp^3 of < 0.5 . In this context, optimal Fsp^3 values (0.21–0.32) were found for **8–9(a–d)**. Further, the number of aromatic and heteroaromatic rings (#ArRNG) was also taken into consideration. Note that our hybrids contained three aromatic rings (~96% of marketed drugs meet this criterion), which means they have better chances during drug development [42]. Lastly, we employed pan-assay interference compound (PAINS) filters on compounds **8–9(a–d)** in order to examine possible early warning indications of toxicity [44]. This analysis showed that there were no PAINS alerts for any compounds. Altogether, according to the computed data, an ideal pharmacokinetic profile appears to be produced when 5-FU and coumarin/chromone fragments are combined into a unique structural core. *In silico* results allowed us to infer that this innovative hybrid scaffold should be taken into account for subsequent biological investigations.

3. Materials and Methods

3.1. Chemical Synthesis

5-FU ($\geq 98.0\%$) was purchased from AK scientific and chemicals (Union City, CA, USA). Coumarin and chromone were obtained following the methods reported elsewhere [45,46]. In sealed vessels, microwave reactions were conducted using a CEM Discover microwave reactor (maximum power of 300 W, temperature control via infrared sensor, and constant temperature). The reactions were aided by the use of BRANSON ultrasound technology. An AMX 300 device (Bruker, Billerica, MA, USA) running at 300 MHz for 1H and 75 MHz for ^{13}C was used to record the NMR spectra. The chemical shifts (δ) were shown in parts per million (ppm) and the signals of the deuterated solvents served as references. TMS served as the internal benchmark. Coupling constants (J) are given in Hertz (Hz). Using a Bruker Impact II UHR-Q-TOF mass spectrometer in positive mode (Bruker Daltonik GmbH, Bremen, Germany), HRMS was obtained.

General Procedure for the synthesis of bromoalkyl derivatives **3a–d** and **4a–d**.

A mixture of 1 mmol of coumarin or chromone, 1.5 mmol of K_2CO_3 , and 10 mL of acetone was added to a 25 mL flask with a flat bottom and a magnetic stirring bar. The mixture was then stirred for 30 min. After adding 1.2 mmol of 1, ω -dibromoalkane, the mixture was sonicated for one hour at $25^\circ C$. This was followed by the addition of water, the transfer of the mixture to a separating funnel, and extraction with ethyl acetate. The organic phase was dried with anhydrous sodium sulfate. The liquid phase was concentrated using a rotatory evaporator at low pressure, and the residue was purified using flash chromatography on silica gel with an eluent combination of varying ratios of hexanes and ethyl acetate. Bromoalkyl derivatives were obtained in yields ranging between 66 and 71% for **3a–d** and 70 and 76% for **4a–d**.

7-(3-bromopropoxy)-2H-chromen-2-one (3a): Orange oil; yield: 68%; 1H NMR (300 MHz, Chloroform-*d*) δ 7.68 (d, $J = 9.5$ Hz, 1H), 7.42 (d, $J = 8.3$ Hz, 1H), 6.91–6.85 (m, 2H), 6.30 (d, $J = 9.5$ Hz, 1H), 4.21 (t, $J = 5.8$ Hz, 2H), 3.65 (t, $J = 6.4$ Hz, 2H), 2.46–2.34 (m, 2H). ^{13}C NMR (75 MHz, Chloroform-*d*) δ 161.88 (Ar-O-), 161.23 (C=O), 155.85 (Ar-O-), 143.44, 128.87, 113.27, 112.79, 112.75, 101.55, 65.88 (-OCH₂-), 31.97, 29.64 (-CH₂-Br).

7-(4-bromobutoxy)-2H-chromen-2-one (3b): Orange oil; yield: 71%; 1H NMR (300 MHz, Chloroform-*d*) δ 7.68 (d, $J = 9.5$ Hz, 1H), 7.41 (d, $J = 8.5$ Hz, 1H), 6.90–6.82 (m, 2H), 6.29 (d, $J = 9.5$ Hz, 1H), 4.10 (t, $J = 5.8$ Hz, 2H), 3.54 (t, $J = 6.3$ Hz, 2H), 2.19–1.97 (m, 4H). ^{13}C NMR (75 MHz, Chloroform-*d*) δ 162.08 (Ar-O), 161.27 (C=O), 155.89 (Ar-O), 143.47, 132.52, 128.82, 113.14, 112.90, 112.59, 101.87, 101.35, 67.54 (-CH₂-O-), 33.29 (-CH₂-Br), 29.33, 27.67.

7-((5-bromopentyl)oxy)-2H-chromen-2-one (3c): Orange oil; yield: 68%; 1H NMR (300 MHz, Chloroform-*d*) δ 7.68 (d, $J = 9.5$ Hz, 1H), 7.41 (d, $J = 8.5$ Hz, 1H), 6.91–6.81 (m,

2H), 6.29 (d, J = 9.5 Hz, 1H), 4.07 (t, J = 6.3 Hz, 2H), 3.49 (t, J = 6.7 Hz, 2H), 2.06–1.83 (m, 5H), 1.81–1.63 (m, 2H). ^{13}C NMR (75 MHz, Chloroform-*d*) δ 162.23 (Ar-O), 161.33 (C=O), 155.90 (Ar-O), 143.52, 128.79, 113.04, 112.97, 112.50, 101.33, 68.24 (-CH₂-O-), 33.56 (-CH₂-Br), 32.40, 28.20, 24.77.

7-((6-bromohexyl)oxy)-2*H*-chromen-2-one (3d**):** Orange oil; yield: 66%; ^1H NMR (300 MHz, Chloroform-*d*) δ 7.68 (d, J = 9.5 Hz, 1H), 7.41 (d, J = 8.5 Hz, 1H), 6.92–6.82 (m, 2H), 6.29 (d, J = 9.5 Hz, 1H), 4.06 (t, J = 6.4 Hz, 2H), 3.48 (t, J = 6.7 Hz, 2H), 2.03–1.81 (m, 2H), 1.72–1.49 (m, 6H). ^{13}C NMR (75 MHz, Chloroform-*d*) δ 162.33 (Ar-O), 161.35 (C=O), 155.92 (Ar-O), 143.51, 128.76, 113.00 (2C), 112.46, 101.32, 68.40 (-CH₂-O-), 33.81 (-CH₂-Br), 32.63, 28.84, 27.90, 25.26.

7-(3-bromopropoxy)-4*H*-chromen-4-one (4a**):** Orange solid; yield: 76%; mp: 91–93 °C; ^1H NMR (300 MHz, Chloroform-*d*) δ 7.68 (d, J = 9.5 Hz, 1H), 7.41 (d, J = 8.5 Hz, 1H), 6.87 (dd, J = 8.5, 2.4 Hz, 1H), 6.83 (d, J = 2.4 Hz, 1H), 6.29 (d, J = 9.5 Hz, 1H), 4.24 (t, J = 5.8 Hz, 2H), 3.66 (t, J = 6.3 Hz, 2H), 2.46–2.36 (m, 2H). ^{13}C NMR (75 MHz, Chloroform-*d*) δ 177.06 (C=O), 163.14 (Ar-O-), 158.21 (Ar-O-), 154.95 (-CH=CH-O-), 127.31, 118.94, 114.77, 112.99, 101.02, 65.92 (-CH₂-O-), 31.94 (-CH₂-Br), 29.63.

7-(4-bromobutoxy)-4*H*-chromen-4-one (4b**):** Orange solid; yield: 74%; mp: 89–92 °C; ^1H NMR (300 MHz, Chloroform-*d*) δ 8.14 (d, J = 8.9 Hz, 1H), 7.82 (d, J = 6.0 Hz, 1H), 7.00 (dd, J = 8.9, 2.4 Hz, 1H), 6.86 (d, J = 2.4 Hz, 1H), 6.32 (d, J = 6.0 Hz, 1H), 4.13 (t, J = 5.8 Hz, 2H), 3.54 (t, J = 6.2 Hz, 2H), 2.20–1.98 (m, 4H). ^{13}C NMR (75 MHz, Chloroform-*d*) δ 177.09 (C=O), 163.35 (Ar-O-), 158.24 (Ar-O-), 154.91 (-CH=CH-O-), 127.26, 118.80, 114.79, 112.97, 100.89, 67.57 (-CH₂-O-), 33.26 (-CH₂-Br), 29.29, 27.63.

7-((5-bromopentyl)oxy)-4*H*-chromen-4-one (4c**):** Orange solid; yield: 72%; mp: 80–82 °C; ^1H NMR (300 MHz, Chloroform-*d*) δ 8.14 (d, J = 8.9 Hz, 1H), 7.82 (d, J = 6.0 Hz, 1H), 7.00 (dd, J = 8.9, 2.4 Hz, 1H), 6.86 (d, J = 2.3 Hz, 1H), 6.32 (d, J = 6.0 Hz, 1H), 4.10 (t, J = 6.3 Hz, 2H), 3.49 (t, J = 6.7 Hz, 2H), 2.06–1.84 (m, 4H), 1.83–1.63 (m, 2H). ^{13}C NMR (75 MHz, Chloroform-*d*) δ 177.11 (C=O), 163.49 (Ar-O-), 158.25 (Ar-O-), 154.89 (-CH=CH-O-), 127.21, 118.71, 114.83, 112.95, 100.87, 68.29 (-CH₂-O-), 33.53 (-CH₂-Br), 32.38, 28.19, 24.76.

7-((6-bromohexyl)oxy)-4*H*-chromen-4-one (4d**):** Orange solid; yield: 70%; mp: 65–68 °C; ^1H NMR (300 MHz, Chloroform-*d*) δ 8.14 (d, J = 8.9 Hz, 1H), 7.82 (d, J = 6.0 Hz, 1H), 6.99 (dd, J = 8.9, 2.4 Hz, 1H), 6.86 (d, J = 2.4 Hz, 1H), 6.31 (d, J = 6.0 Hz, 1H), 4.08 (t, J = 6.5 Hz, 2H), 3.47 (t, J = 6.7 Hz, 2H), 2.02–1.81 (m, 6H), 1.62–1.48 (m, 2H). ^{13}C NMR (75 MHz, Chloroform-*d*) δ 177.12 (C=O), 163.58 (Ar-O-), 158.27 (Ar-O-), 154.89 (-CH=CH-O-), 127.18, 118.66, 114.86, 112.94, 100.85, 68.44 (-CH₂-O-), 33.81 (-CH₂-Br), 32.62, 28.82, 27.87, 25.24.

General Procedure for the Synthesis of Alkyl Azide Derivatives **5a–d** and **6a–d**.

A 10 mL flask with a flat bottom and a magnetic stirring bar was filled with compounds **3a–d** and **4a–d** (1 mmol), sodium azide (3 mmol), and DMF (5 mL). Following that, the mixture was microwave-heated for 15 min at 200 W to 100 °C. Following the addition of water, the mixture was moved to a separating funnel and ethyl acetate was used for extraction. To dry the organic phase, anhydrous sodium sulfate was utilized. Using a mixture of hexanes/ethyl acetate in varying ratios as the eluent, flash chromatography was used to purify the residue after the liquid phase was concentrated under decreased pressure on a rotatory evaporator. Alkyl azide derivatives were obtained in yields ranging from 64 to 70% yields for **5a–d** and 67 to 72% yields for chromone-alkyl azides **6a–d**.

7-(3-azidopropoxy)-2*H*-chromen-2-one (5a**):** Orange oil; yield: 70%; ^1H NMR (300 MHz, Chloroform-*d*) δ 7.68 (d, J = 9.5 Hz, 1H), 7.42 (d, J = 8.5 Hz, 1H), 6.97–6.79 (m, 2H), 6.29 (dd, J = 9.4, 1.6 Hz, 1H), 4.15 (t, J = 5.9 Hz, 2H), 3.58 (t, J = 6.5 Hz, 2H), 2.20–2.05 (m, 2H). ^{13}C NMR (75 MHz, Chloroform-*d*) δ 161.85 (C=O), 161.25 (Ar-O-), 155.84 (Ar-O-), 143.46, 128.88, 113.25, 112.81, 112.74, 101.47, 65.13 (-CH₂O-), 48.04 (-CH₂N₃), 28.56.

7-(4-azidobutoxy)-2*H*-chromen-2-one (5b**):** Orange oil; yield: 67%; ^1H NMR (300 MHz, Chloroform-*d*) δ 7.68 (d, J = 9.5 Hz, 1H), 7.41 (d, J = 8.6 Hz, 1H), 6.91–6.82 (m, 2H), 6.29 (d, J = 9.5 Hz, 1H), 4.09 (t, J = 5.9 Hz, 2H), 3.43 (t, J = 6.5 Hz, 2H), 2.03–1.73 (m, 4H). ^{13}C NMR (75 MHz, Chloroform-*d*) δ 162.09 (C=O), 161.28 (Ar-O-), 155.88 (Ar-O-), 143.49, 128.83, 113.12, 112.92, 112.58, 101.33, 67.85 (-CH₂O-), 51.13 (-CH₂N₃), 26.31, 25.69.

7-((5-azidopentyl)oxy)-2H-chromen-2-one (5c): Orange oil; yield: 65%; ^1H NMR (300 MHz, Chloroform-d) δ 7.68 (d, J = 9.5 Hz, 1H), 7.41 (d, J = 8.5 Hz, 1H), 6.91–6.80 (m, 2H), 6.28 (d, J = 9.5 Hz, 1H), 4.06 (t, J = 6.3 Hz, 2H), 3.36 (t, J = 6.5 Hz, 2H), 1.89 (dp, J = 19.4, 7.0 Hz, 4H), 1.79–1.54 (m, 2H). ^{13}C NMR (75 MHz, Chloroform-d) δ 162.24 (C=O), 161.33 (Ar-O-), 155.90 (Ar-O-), 143.52, 128.80, 113.03, 112.97, 112.50, 101.31, 68.24 (-CH₂O-), 51.31 (-CH₂N₃), 28.64, 28.58, 23.36.

7-((6-azidohexyl)oxy)-2H-chromen-2-one (5d): Orange oil; yield: 64%; ^1H NMR (300 MHz, Chloroform-d) δ 7.68 (d, J = 9.5 Hz, 1H), 7.41 (d, J = 8.5 Hz, 1H), 6.92–6.81 (m, 2H), 6.29 (d, J = 9.5 Hz, 1H), 4.06 (t, J = 6.3 Hz, 2H), 3.34 (t, J = 6.8 Hz, 2H), 1.95–1.81 (m, 2H), 1.77–1.63 (m, 2H), 1.62–1.43 (m, 4H). ^{13}C NMR (75 MHz, Chloroform-d) δ 162.32 (C=O), 161.34 (Ar-O-), 155.92 (Ar-O-), 143.52, 128.77, 112.99 (2C), 112.46, 101.31, 68.39 (-CH₂O-), 51.37 (-CH₂N₃), 28.88, 28.81, 26.50, 25.65.

7-(3-azidopropoxy)-4H-chromen-4-one (6a): Orange oil; yield: 72%; ^1H NMR (300 MHz, Chloroform-d) δ 7.68 (d, J = 9.5 Hz, 1H), 7.41 (d, J = 8.5 Hz, 1H), 6.87 (dd, J = 8.5, 2.4 Hz, 1H), 6.83 (d, J = 2.4 Hz, 1H), 6.29 (d, J = 9.5 Hz, 1H), 4.07 (t, J = 6.3 Hz, 2H), 3.49 (t, J = 6.7 Hz, 2H), 2.06–1.83 (m, 4H), 1.79–1.62 (m, 2H). ^{13}C NMR (75 MHz, Chloroform-d) δ 177.22 (C=O), 163.18 (Ar-O-), 158.24 (Ar-O-), 155.06 (-CH=CH-O-), 127.33, 118.86, 114.83, 112.92, 100.99, 65.19 (-CH₂O-), 48.01 (-CH₂-Br), 31.00, 28.54.

7-(4-azidobutoxy)-4H-chromen-4-one (6b): Orange oil; yield: 70%; ^1H NMR (300 MHz, Chloroform-d) δ 8.15 (d, J = 8.7 Hz, 1H), 7.83 (d, J = 6.0 Hz, 1H), 7.00 (d_{app} , J = 8.9 Hz, 1H), 6.86 (s_{app} , 1H), 6.33 (d, J = 6.0 Hz, 1H), 4.12 (t, J = 6.0 Hz, 2H), 3.43 (t, J = 6.2 Hz, 2H), 2.20–1.98 (m, 4H). ^{13}C NMR (75 MHz, Chloroform-d) δ 177.20 (C=O), 163.40 (Ar-O-), 158.26 (Ar-O-), 155.00 (-CH=CH-O-), 127.26, 118.74, 114.84, 112.92, 100.90, 67.90 (-CH₂O-), 51.11 (-CH₂-Br), 26.29, 25.67.

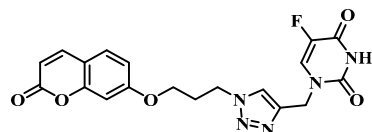
7-((5-azidopentyl)oxy)-4H-chromen-4-one (6c): Orange oil; yield: 69%; ^1H NMR (300 MHz, Chloroform-d) δ 8.14 (d, J = 8.9 Hz, 1H), 7.82 (d, J = 6.1 Hz, 1H), 7.00 (dd, J = 8.9, 2.4 Hz, 1H), 6.86 (d, J = 2.4 Hz, 1H), 6.32 (d, J = 6.0 Hz, 1H), 4.09 (t, J = 6.3 Hz, 2H), 3.37 (t, J = 6.6 Hz, 2H), 1.97–1.80 (m, 4H), 1.77–1.55 (m, 2H). ^{13}C NMR (75 MHz, Chloroform-d) δ 177.16 (C=O), 163.51 (Ar-O-), 158.27 (Ar-O-), 154.93 (-CH=CH-O-), 127.21, 118.69, 114.85, 112.93, 100.86, 68.29 (-CH₂O-), 51.31 (-CH₂-Br), 30.99, 28.63, 23.36.

7-((6-azidohexyl)oxy)-4H-chromen-4-one (6d): Orange oil; yield: 67%; ^1H NMR (300 MHz, Chloroform-d) δ 8.14 (d, J = 8.9 Hz, 1H), 7.82 (d, J = 6.0 Hz, 1H), 7.00 (dd, J = 8.9, 2.4 Hz, 1H), 6.86 (d, J = 2.4 Hz, 1H), 6.31 (d, J = 6.0 Hz, 1H), 4.08 (t, J = 6.4 Hz, 2H), 3.34 (t, J = 6.8 Hz, 2H), 1.95–1.79 (m, 4H), 1.77–1.63 (m, J = 6.8 Hz, 2H), 1.61–1.45 (m, 4H). ^{13}C NMR (75 MHz, Chloroform-d) δ 177.13 (C=O), 163.58 (Ar-O-), 158.27 (Ar-O-), 154.89 (-CH=CH-O-), 130.64, 127.18, 114.86, 112.93, 100.84, 68.43 (-CH₂O-), 51.37 (-CH₂-Br), 28.87, 28.81, 26.49, 25.64.

General procedure for the synthesis of 5-FU-Coumarin (**8a–d**) and 5-FU-Chromone hybrids (**9a–d**) was as follows: hybrids were synthesized according to the following procedure [7].

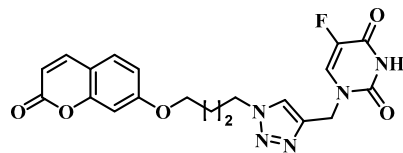
Coumarin-alkyl azides (**5a–d**) or chromone-alkyl azides (**6a–d**) (1 mmol), propargyl-5-FU (**7**) [25] (1 mmol), and DMF (5 mL) were added to a 10 mL flask with a flat bottom. The mixture was then sonicated for five minutes at 40 °C. Following this, 0.5 mmol of ascorbic acid, 0.5 mmol of copper acetate, 1 mL of DMF, and 1 mL of water were added, and the reaction mixture was sonicated for 1 h at 40 °C. Next, 10% HCl was applied, and ethyl acetate was used for extraction. After the organic phase was dried on anhydrous sodium sulfate, it was filtered, concentrated under reduced pressure, and the residue was crystallized in a 1:1 ratio of MeOH to H₂O. Finally, the solid obtained was purified by preparative chromatography on silica gel to obtain compounds **8a–d** and **9a–d**. The ^1H , ^{13}C NMR, and MS spectra of all hybrids can be found in the Supplementary Materials.

5-fluoro-1-((1-(3-((2-oxo-2H-chromen-7-yl)oxy)propyl)-1*H*-1,2,3-triazol-4-yl)methyl) pyrimidine-2,4(1*H*,3*H*)-dione (8a):



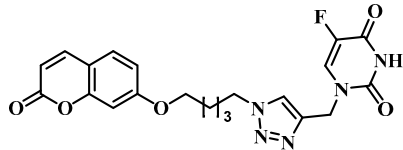
Pale-yellow solid; yield: 71%; mp: 175–178 °C; ^1H NMR (300 MHz, DMSO-d₆) δ 8.17 (d, J = 6.5 Hz, 2H), 7.99 (d, J = 9.5 Hz, 1H), 7.62 (d, J = 8.6 Hz, 1H), 6.97 (d, J = 2.4 Hz, 1H), 6.90 (dd, J = 8.6, 2.4 Hz, 1H), 6.29 (d, J = 9.5 Hz, 1H), 4.90 (s, 2H), 4.53 (t, J = 6.9 Hz, 2H), 4.09 (t, J = 6.0 Hz, 2H), 2.30 (p , J = 6.6 Hz, 2H). ^{13}C NMR (75 MHz, DMSO-d₆) δ 161.88 (Ar-O), 160.76 (C=O, coumarin), 158.08 and 157.74 (F-C-C=O), 155.78 (Ar-O), 149.82 (N-C=O), 144.79, 142.64 (triazolyl), 141.61 and 138.57 (F-C), 130.61 and 130.17 (CH-C-F), 129.95, 124.18 (triazolyl), 113.14, 113.01, 112.90, 101.62, 65.85 (−CH₂-O-), 47.06 (triazolyl-(N)-CH₂-), 43.18 (5-FU-(N)-CH₂-), 29.60. HRMS (ESI) calcd for C₁₉H₁₆FN₅O₅ [M+H]⁺: 414.1226; found: 414.1229.

5-fluoro-1-((1-(4-((2-oxo-2H-chromen-7-yl)oxy)butyl)-1H-1,2,3-triazol-4-yl)methyl)pyrimidine-2,4(1H,3H)-dione (**8b**):



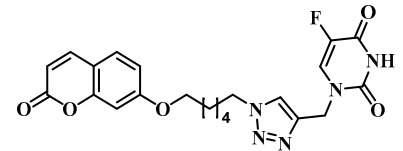
Pale-yellow solid; yield: 90%; mp: 172–175 °C; ^1H NMR (300 MHz, DMSO-d₆) δ 8.19 (d, J = 6.7 Hz, 1H), 8.14 (s, 1H), 7.99 (d, J = 9.5 Hz, 1H), 7.62 (d, J = 8.6 Hz, 1H), 6.98 (d, J = 2.4 Hz, 1H), 6.93 (dd, J = 8.6, 2.4 Hz, 1H), 6.28 (d, J = 9.5 Hz, 1H), 4.90 (s, 2H), 4.42 (t, J = 7.0 Hz, 2H), 4.09 (t, J = 6.3 Hz, 2H), 2.04–1.89 (m, 2H), 1.78–1.63 (m, 2H). ^{13}C NMR (75 MHz, DMSO-d₆) δ 162.15 (Ar-O), 160.76 (C=O, coumarin), 158.09 and 157.74 (F-C-C=O), 155.84 (Ar-O), 149.84 (N-C=O), 144.81, 142.60 (triazolyl), 141.62 and 138.59 (F-C), 130.65 and 130.20 (CH-C-F), 129.94, 124.00 (triazolyl), 113.17, 112.91, 112.78, 101.61, 68.05 (−CH₂-O-), 49.51 (triazolyl-(N)-CH₂-), 43.24 (5-FU-(N)-CH₂-), 26.87, 25.90. HRMS (ESI) calcd for C₂₀H₁₈FN₅O₅ [M+H]⁺: 428.1416; found: 428.1420.

5-fluoro-1-((1-(5-((2-oxo-2H-chromen-7-yl)oxy)pentyl)-1H-1,2,3-triazol-4-yl)methyl)pyrimidine-2,4(1H,3H)-dione (**8c**):



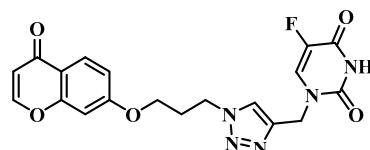
Pale-yellow solid; yield: 96%; mp: 164–166 °C; ^1H NMR (600 MHz, DMSO-d₆) δ 8.17 (d, J = 6.6 Hz, 1H), 8.12 (s, 1H), 7.98 (d, J = 9.5 Hz, 1H), 7.61 (d, J = 8.6 Hz, 1H), 6.96 (d, J = 2.4 Hz, 1H), 6.91 (dd, J = 8.6, 2.4 Hz, 1H), 6.28 (d, J = 9.5 Hz, 1H), 4.90 (s, 2H), 4.37 (t, J = 7.1 Hz, 2H), 4.06 (t, J = 6.4 Hz, 2H), 1.88 (p , J = 7.3 Hz, 2H), 1.76 (p , J = 6.7 Hz, 2H), 1.43–1.36 (m, 2H). ^{13}C NMR (75 MHz, DMSO-d₆) δ 162.24 (Ar-O), 160.78 (C=O, coumarin), 158.09 and 157.75 (F-C-C=O), 155.85 (Ar-O), 149.83 (N-C=O), 144.81, 142.54 (triazolyl), 141.62 and 138.58 (F-C), 130.64 and 130.19 (CH-C-F), 129.92, 123.92 (triazolyl), 113.18, 112.84, 112.71, 101.55, 68.48 (−CH₂-O-), 49.76 (triazolyl-(N)-CH₂-), 43.23 (5-FU-(N)-CH₂-), 29.78, 28.22, 22.90. HRMS (ESI) calcd for C₂₁H₂₀FN₅O₅ [M+H]⁺: 442.1512; found: 442.1516.

5-fluoro-1-((1-(6-((2-oxo-2H-chromen-7-yl)oxy)hexyl)-1H-1,2,3-triazol-4-yl)methyl)pyrimidine-2,4(1H,3H)-dione (**8d**):



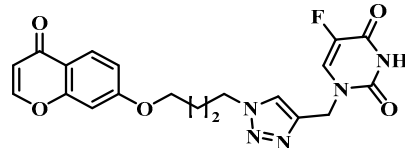
Pale-yellow solid; yield: 90%; mp: 160–163 °C; ^1H NMR (300 MHz, DMSO-d₆) δ 8.18 (d, J = 6.6 Hz, 1H), 8.13 (s, 1H), 7.98 (d, J = 9.5 Hz, 1H), 7.61 (d, J = 8.5 Hz, 1H), 6.96 (d, J = 2.4 Hz, 1H), 6.92 (dd, J = 8.5, 2.4 Hz, 1H), 6.27 (d, J = 9.5 Hz, 1H), 4.89 (s, 2H), 4.33 (t, J = 7.1 Hz, 2H), 4.04 (t, J = 6.3 Hz, 2H), 1.89–1.76 (m, 2H), 1.75–1.64 (m, 2H), 1.49–1.36 (m, 2H), 1.35–1.20 (m, 2H). ^{13}C NMR (75 MHz, DMSO-d₆) δ 162.28 (Ar-O), 160.80 (C=O, coumarin), 158.09 and 157.75 (F-C-C=O), 155.85, 149.82, 144.82 (triazolyl), 141.60 and 138.59 (F-C), 130.63 and 130.20 (CH-C-F), 130.20, 129.93, 123.94 (triazolyl), 113.16, 112.82, 112.68, 101.54, 68.60 (-CH₂-O-), 49.83 (triazolyl-(N)-CH₂-), 43.26 (5-FU-(N)-CH₂-), 29.99, 28.66, 26.00, 25.28. HRMS (ESI) calcd for C₂₂H₂₂FN₅O₅ [M+H]⁺: 456.1687; found: 456.1690.

5-fluoro-1-((1-(3-((4-oxo-4H-chromen-7-yl)oxy)propyl)-1*H*-1,2,3-triazol-4-yl)methyl) pyrimidine-2,4(1*H*,3*H*)-dione (**9a**):



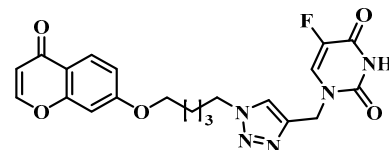
Pale-yellow solid; yield: 70%; mp: 186–188 °C; ^1H NMR (300 MHz, DMSO-d₆) δ 8.21 (d, J = 6.1 Hz, 1H), 8.19–8.15 (m, 2H), 7.92 (d, J = 8.8 Hz, 1H), 7.08 (d, J = 2.3 Hz, 1H), 7.00 (dd, J = 8.8, 2.3 Hz, 1H), 6.27 (d, J = 6.1 Hz, 1H), 4.90 (s, 2H), 4.54 (t, J = 6.9 Hz, 2H), 4.13 (t, J = 5.9 Hz, 2H), 2.31 (p, J = 6.5 Hz, 2H). ^{13}C NMR (75 MHz, DMSO-d₆) δ 176.13 (C=O, chromone), 163.18 (Ar-O), 158.15 (-CH=CH-O-), 158.08 and 157.75 (F-C-C=O), 156.96, 149.84 (N-C=O), 141.62 and 138.58 (F-C), 130.62 and 130.17 (CH-C-F), 126.87 (triazolyl), 124.27 (triazolyl), 118.57, 115.31, 112.61, 101.77, 66.08 (-CH₂-O-), 47.14 (triazolyl-(N)-CH₂-), 43.20 (5-FU-(N)-CH₂-), 29.53. HRMS (ESI) calcd for C₁₉H₁₆FN₅O₅ [M+H]⁺: 414.1186; found: 414.1188.

5-fluoro-1-((1-(4-((4-oxo-4H-chromen-7-yl)oxy)butyl)-1*H*-1,2,3-triazol-4-yl)methyl) pyrimidine-2,4(1*H*,3*H*)-dione (**9b**):



Pale-yellow solid; yield: 82%; mp: 168–170 °C; ^1H NMR (300 MHz, DMSO-d₆) δ 11.86 (N-H), 8.27–8.08 (m, 3H), 7.92 (d, J = 8.8 Hz, 1H), 7.11 (d, J = 2.3 Hz, 1H), 7.04 (dd, J = 8.8, 2.3 Hz, 1H), 6.26 (d, J = 6.0 Hz, 1H), 4.90 (s, 2H), 4.43 (t, J = 7.0 Hz, 2H), 4.12 (t, J = 6.3 Hz, 2H), 2.05–1.89 (m, 2H), 1.79–1.64 (m, 2H). ^{13}C NMR (75 MHz, DMSO-d₆) δ 176.13 (C=O, chromone), 163.43 (Ar-O), 158.20 (-CH=CH-O-), 158.08 and 157.74 (F-C-C=O), 156.94, 149.84 (N-C=O), 141.62 and 138.52 (F-C), 130.67 and 130.21 (CH-C-F), 126.83 (triazolyl), 124.18 (triazolyl), 118.46, 115.39, 112.61, 101.74, 68.21 (-CH₂-O-), 49.53 (triazolyl-(N)-CH₂-), 43.27 (5-FU-(N)-CH₂-), 26.84, 25.85. HRMS (ESI) calcd for C₂₀H₁₈FN₅O₅ [M+H]⁺: 428.1347; found: 428.1350.

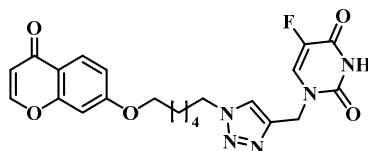
5-fluoro-1-((1-(5-((4-oxo-4H-chromen-7-yl)oxy)pentyl)-1*H*-1,2,3-triazol-4-yl)methyl) pyrimidine-2,4(1*H*,3*H*)-dione (**9c**):



Pale-yellow solid; yield: 92%; mp: 160–163 °C; ^1H NMR (300 MHz, DMSO-d₆) δ 11.86 (N-H), 8.26–8.10 (m, 3H), 7.92 (d, J = 8.8 Hz, 1H), 7.10 (d, J = 2.3 Hz, 1H), 7.02 (dd, J = 8.8,

2.3 Hz, 1H), 6.26 (d, J = 6.0 Hz, 1H), 4.89 (s, 2H), 4.37 (t, J = 7.1 Hz, 2H), 4.08 (t, J = 6.4 Hz, 2H), 1.94–1.82 (m, 2H), 1.81–1.71 (m, 2H), 1.46–1.42 (m, 2H). ^{13}C NMR (75 MHz, DMSO-d₆) δ 176.13 (C=O, chromone), 163.53 (Ar-O), 158.22 (-CH=CH-O-), 158.09 and 157.74 (F-C=C=O), 156.92, 149.83 (N-C=O), 141.55–138.51 (F-C), 130.65 and 130.18 (CH-C-F), 126.81 (triazolyl), 124.00 (triazolyl), 118.41, 115.39, 112.60, 101.69, 68.64 (-CH₂-O-), 49.77 (triazolyl-(N)-CH₂), 43.25 (5-FU-(N)-CH₂), 29.75, 28.16, 22.88. HRMS (ESI) calcd for C₂₁H₂₀FN₅O₅ [M+H]⁺: 442.1505; found: 442.1509.

5-fluoro-1-((1-(6-((4-oxo-4H-chromen-7-yl)oxy)hexyl)-1*H*-1,2,3-triazol-4-yl)methyl)pyrimidine-2,4(1*H*,3*H*)-dione (**9d**):



Pale-yellow solid; yield: 90%; mp: 156–158 °C; ^1H NMR (300 MHz, DMSO-d₆) δ 11.84 (N-H), 8.23–8.09 (m, 3H), 7.92 (d, J = 8.9 Hz, 1H), 7.10 (d, J = 2.4 Hz, 1H), 7.03 (dd, J = 8.9, 2.4 Hz, 1H), 6.26 (d, J = 6.0 Hz, 1H), 4.89 (s, 2H), 4.33 (t, J = 7.0 Hz, 2H), 4.07 (t, J = 6.3 Hz, 2H), 1.92–1.77 (m, 2H), 1.76–1.63 (m, 2H), 1.49–1.36 (m, 2H), 1.35–1.18 (m, 2H). ^{13}C NMR (75 MHz, DMSO-d₆) δ 176.16 (C=O, chromone), 163.57 (Ar-O), 158.23 (-CH=CH-O-), 156.93, 149.83 (N-C=O), 158.09 and 157.72 (F-C-C=O), 141.50 and 138.43 (F-C), 130.94 and 130.19 (CH-C-F), 126.82 (triazolyl), 123.57 (triazolyl), 118.38, 115.40, 112.59, 101.67, 68.78 (-CH₂-O-), 49.82 (triazolyl-(N)-CH₂), 43.14 (5-FU-(N)-CH₂), 29.99, 28.61, 26.00, 25.27. HRMS (ESI) calcd for C₂₂H₂₂FN₅O₅ [M+H]⁺: 456.1685; found: 456.1688.

3.2. Theoretical Drug-Likeness Studies

Novel hybrids **8–9(a–d)** were screened for their pharmacokinetic properties using the opensource SwissADME cheminformatics toolkits [47]. For **8–9(a–d)**, eleven relevant biopharmaceutical properties were accessed: topographical polar surface area (TPSA), MW and rotatable bonds, log P_{o/w}, binding to human serum albumin (logK_{HSA}), apparent predicted intestinal permeability (App. Caco-2 and MDCK models), the fraction of sp³ carbon atoms, and the number of aromatic/heteroaromatic rings. Finally, SwissADME was also used to investigate substructural alerts to identify pan-assay interference compounds (PAINS). The fact that these vital biopharmaceutical indices control oral exposure, absorption, motility, and permeability of novel drugs candidates is noteworthy.

4. Conclusions

In this work, we synthesized eight new hybrids based on 5-FU (four 5-fluorouracil-coumarin and 5-fluorouracil-chromone hybrids), using Huisgen 1,3-dipolar cycloaddition, a type of click chemistry, as the key step, with good yields. These compounds and the intermediates of synthesis were characterized by spectroscopic analysis. Afterward, computer-aided prediction of the drug-like and pharmacokinetic indices for hybrids **8–9(a–d)** suggested that this class of compounds would tend to have favorable biopharmaceutical parameters, making them eligible for entry in further biological studies.

Supplementary Materials: Supplementary data (^1H , ^{13}C NMR and MS spectra of all hybrids (**8a–d** and **9a–d**) associated with this article) can be found in the online version. The supplementary data include the following: Figure S1a: ^1H NMR of compound **8a**, Figure S1b: ^{13}C NMR of compound **8a** and Figure S1c: MS spectra of compound **8a**; Figure S2a: ^1H NMR of compound **8b**, Figure S2b: ^{13}C NMR of compound **8b** and Figure S2c: MS spectra of compound **8b**; Figure S3a: ^1H NMR of compound **8c**, Figure S3b: ^{13}C NMR of compound **8c** and Figure S3c: MS spectra of compound **8c**; Figure S4a: ^1H NMR of compound **8d**, Figure S4b: ^{13}C NMR of compound **8d** and Figure S4c: MS spectra of compound **8d**; Figure S5a: ^1H NMR of compound **9a**, Figure S5b: ^{13}C NMR of compound **9a** and Figure S5c: MS spectra of compound **9a**; Figure S6a: ^1H NMR of compound **9b**, Figure S6b: ^{13}C NMR of compound **9b** and Figure S6c: MS spectra of compound **9b**; Figure S7a: ^1H NMR of

compound **9c**, Figure S7b: ^{13}C NMR of compound **9c** and Figure S7c: MS spectra of compound **9c**; Figure S8a: ^1H NMR of compound **9d**, Figure S8b: ^{13}C NMR of compound **9d** and Figure S8c: MS spectra of compound **9d**.

Author Contributions: L.G.-A.: synthesis and characterization of hybrid molecules. A.F.Y.: in silico studies, analysis, writing—original draft. W.C.-G.: resources, supervision, project administration, funding acquisition, writing—original draft, writing—review and editing. All authors have read and agreed to the published version of the manuscript.

Funding: This research was funded by the University of Antioquia and the Ministry of Science MINCIENCIAS through the program NanoBioCáncer 2.0 GAT 2.0; código: 121092092332, grant: 621-2022, project number: 92355.

Data Availability Statement: The data presented in this study are available in this article and the Supplementary Materials.

Acknowledgments: The authors thank the University of Antioquia and MINCIENCIAS for their support.

Conflicts of Interest: The authors declare no conflicts of interest.

References

- Reis, J.; Gaspar, A.; Milhazes, N.; Borges, F. Chromone as a Privileged Scaffold in Drug Discovery: Recent Advances. *J. Med. Chem.* **2017**, *60*, 7941–7957. [[CrossRef](#)] [[PubMed](#)]
- Mohsin, N.U.A.; Irfan, M.; Hassan, S.U.; Saleem, U. Current Strategies in Development of New Chromone Derivatives with Diversified Pharmacological Activities: A Review. *Pharm. Chem. J.* **2020**, *54*, 241–257. [[CrossRef](#)] [[PubMed](#)]
- Annunziata, F.; Pinna, C.; Dallavalle, S.; Tamborini, L.; Pinto, A. An Overview of Coumarin as a Versatile and Readily Accessible Scaffold with Broad-Ranging Biological Activities. *Int. J. Mol. Sci.* **2020**, *21*, 4618. [[CrossRef](#)] [[PubMed](#)]
- Sandhu, S.; Bansal, Y.; Silakari, O.; Bansal, G. Coumarin hybrids as novel therapeutic agents. *Bioorg. Med. Chem.* **2014**, *22*, 3806–3814. [[CrossRef](#)] [[PubMed](#)]
- Duan, Y.D.; Jiang, Y.Y.; Guo, F.X.; Chen, L.X.; Xu, L.L.; Zhang, W.; Liu, B. The antitumor activity of naturally occurring chromones: A review. *Fitoterapia* **2019**, *135*, 114–129. [[CrossRef](#)]
- Song, X.F.; Fan, J.; Liu, L.; Liu, X.F.; Gao, F. Coumarin derivatives with anticancer activities: An update. *Arch. Pharm.* **2020**, *353*, e2000025. [[CrossRef](#)]
- Küpeli Akkol, E.; Genç, Y.; Karpuz, B.; Sobarzo-Sánchez, E.; Capasso, R. Coumarins and Coumarin-Related Compounds in Pharmacotherapy of Cancer. *Cancers* **2020**, *12*, 1959. [[CrossRef](#)]
- Al-Warhi, T.; Sabt, A.; Elkaeed, E.B.; Eldehna, W.M. Recent advancements of coumarin-based anticancer agents: An up-to-date review. *Bioorg. Chem.* **2020**, *103*, 104163. [[CrossRef](#)] [[PubMed](#)]
- Banikazemi, Z.; Mirazimi, S.M.; Dashti, F.; Mazandaranian, M.R.; Akbari, M.; Morshedi, K.; Aslanbeigi, F.; Rashidian, A.; Chamanara, M.; Hamblin, M.R.; et al. Coumarins and Gastrointestinal Cancer: A New Therapeutic Option? *Front. Oncol.* **2021**, *11*, 752784. [[CrossRef](#)]
- Herrera, R.A.; Moreno, G.; Araque, P.; Vásquez, I.; Naranjo, E.; Alzate, F.; Cardona, G.W. In-vitro Chemopreventive Potential of a Chromone from Bomarea setacea (ALSTROEMERIACEAE) against Colorectal Cancer. *Iran. J. Pharm. Res.* **2021**, *20*, 254.
- Liu, W.; Hua, J.; Zhou, J.; Zhang, H.; Zhu, H.; Cheng, Y.; Gust, R. Synthesis and in vitro antitumor activity of novel scopoletin derivatives. *Bioorg. Med. Chem. Lett.* **2012**, *22*, 5008. [[CrossRef](#)]
- Kolodziej, H.; Kayser, O.; Woerdenbag, H.J.; van Uden, W.; Pras, N. Structure-cytotoxicity relationships of a series of natural and semi-synthetic simple coumarins as assessed in two human tumour cell lines. *Z. Naturforsch.* **1997**, *52*, 240. [[CrossRef](#)]
- Global Cancer Statistics 2020: GLOBOCAN Estimates of Incidence and Mortality Worldwide for 36 Cancers in 185 Countries. *CA Cancer J. Clin.* **2021**, *71*, 209–249. [[CrossRef](#)]
- Campos, J.; Domínguez, J.F.; Gallo, M.A.; Espinosa, A. From a classic approach in cancer chemotherapy towards differentiation therapy: Acyclic and cyclic seven-membered 5-fluorouracil O,N-acetals. *Curr. Pharm. Des.* **2000**, *18*, 1797–1810. [[CrossRef](#)]
- Cardona, G.W.; Herrera, R.A.; Castrillón, L.W.; Ramírez-Malule, H. Chemistry and Anticancer Activity of Hybrid Molecules and Derivatives based on 5-Fluorouracil. *Curr. Med. Chem.* **2021**, *28*, 5551–5601. [[CrossRef](#)] [[PubMed](#)]
- Keith, C.T.; Borisy, A.; Stockwell, B.R. Multicomponent therapeutics for networked systems. *Nat. Rev. Drug Discov.* **2005**, *4*, 71–78. [[CrossRef](#)]
- Meunier, B. Hybrid molecules with a dual mode of action: Dream or reality? *Acc. Chem. Res.* **2008**, *41*, 69–77. [[CrossRef](#)]
- de Oliveira Pedrosa, M.; Duarte da Cruz, R.M.; de Oliveira Viana, J.; de Moura, R.O.; Ishiki, H.M.; Barbosa Filho, J.M.; Diniz, M.F.; Scotti, M.T.; Scotti, L.; Bezerra Mendonça, F.J. Hybrid Compounds as Direct Multitarget Ligands: A Review. *Curr. Top. Med. Chem.* **2017**, *17*, 1044–1079. [[CrossRef](#)]
- Cardona, G.W.; Yépes, A.F.; Herrera, R.A. Hybrid Molecules: Promising Compounds for the Development of New Treatments Against Leishmaniasis and Chagas Disease. *Curr. Med. Chem.* **2018**, *25*, 3637–3679. [[CrossRef](#)]

20. Kaur, J.; Saxena, M.; Rishi, N. An Overview of Recent Advances in Biomedical Applications of click chemistry. *Bioconjug. Chem.* **2021**, *32*, 1455–1471. [[CrossRef](#)]
21. Li, X.; Xiong, Y. Application of “Click” Chemistry in Biomedical Hydrogels. *ACS Omega* **2022**, *7*, 36918–36928. [[CrossRef](#)] [[PubMed](#)]
22. Kumar, A.; Kumar Yadav, A.; Mishra, V.; Kumar, D. Recent Advancements in Triazole-based click chemistry in Cancer Drug Discovery and Development. *SynOpen* **2023**, *7*, 186–208.
23. Moreno-Quintero, G.; Betancur-Zapata, E.; Herrera-Ramírez, A.; Cardona-Galeano, W. New Hybrid Scaffolds Based on 5-FU/Curcumin: Synthesis, Cytotoxic, Antiproliferative and Pro-Apoptotic Effect. *Pharmaceutics* **2023**, *15*, 1221. [[CrossRef](#)] [[PubMed](#)]
24. Moreno-Quintero, G.; Castrillón-Lopez, W.; Herrera-Ramirez, A.; Yepes-Pérez, A.F.; Quintero-Saumeth, J.; Cardona-Galeano, W. Synthesis and Chemopreventive Potential of 5-FU/Genistein Hybrids on Colorectal Cancer Cells. *Pharmaceutics* **2022**, *15*, 1299. [[CrossRef](#)] [[PubMed](#)]
25. Castrillón-López, W.; Yepes-Pérez, A.F.; Cardona-Galeano, W. Synthesis and In Silico Drug-Likeness Modeling of 5-FU/ASA Hybrids. *Molbank* **2023**, *2023*, M1745. [[CrossRef](#)]
26. Otero, E.; García, E.; Palacios, G.; Yepes, L.M.; Carda, M.; Agut, R.; Vélez, I.D.; Cardona, W.I.; Robledo, S.M. Triclosan-caffeic acid hybrids: Synthesis, leishmanicidal, trypanocidal and cytotoxic activities. *Eur. J. Med. Chem.* **2017**, *141*, 73–83. [[CrossRef](#)]
27. García, E.; Coa, J.C.; Otero, E.; Carda, M.; Vélez, I.D.; Robledo, S.M.; Cardona, W.I. Synthesis and antiprotozoal activity of furanchalcone-quinoline, furanchalcone-chromone and furanchalcone-imidazole hybrids. *Med. Chem. Res.* **2018**, *27*, 497–511. [[CrossRef](#)]
28. Gómez-R, L.; Moreno-Q, G.; Herrera-R, A.; Castrillón-L, W.; Yepes, A.F.; Cardona-Galeano, W. New Hybrid Scaffolds Based on ASA/Genistein: Synthesis, Cytotoxic Effect, Molecular Docking, Drug-likeness and in silico ADME/tox Modeling. *J. Appl. Pharm. Sci.* **2022**, *12*, 15–30.
29. Pessel, F.; Billault, I.; Scherrmann, M.C. Total synthesis of triazole-linked C-glycosyl flavonoids in alternative solvents and environmental assessment in terms of reaction, workup and purification. *Green Chem.* **2016**, *18*, 5558–5568. [[CrossRef](#)]
30. Halay, E.; Ay, E.; Salva, E.; Ay, K.; Karayıldırım, T. Syntheses of 1,2,3-triazole-bridged pyranose sugars with purine and pyrimidine nucleobases and evaluation of their anticancer potential. *Nucleosides Nucleotides Nucleic Acids* **2017**, *36*, 598–619.
31. Shinde, V.; Mhaske, P.C.; Singh, A.; Sarkar, D.; Mahulikar, P. Synthesis and biological evaluation of new 4-(4-(1-benzyl-1H-1,2,3-triazol-4-yl)phenyl)-2-phenyl thiazole derivatives. *J. Heterocycl. Chem.* **2019**, *56*, 3093–3101. [[CrossRef](#)]
32. Ditzinger, F.; Price, D.J.; Ilie, A.R.; Köhl, N.J.; Jankovic, S.; Tsakiridou, G.; Aleandri, S.; Kalantzi, L.; Holm, R.; Nair, A.; et al. Lipophilicity and hydrophobicity considerations in bio-enabling oral formulations approaches—A PEARRL review. *J. Pharm. Pharmacol.* **2019**, *71*, 464–482. [[CrossRef](#)]
33. Pham-The, H.; Cabrera-Pérez, M.Á.; Nam, N.H.; Castillo-Garit, J.A.; Rasulev, B.; Le-Thi-Thu, H.; Casañola-Martin, G.M. In Silico Assessment of ADME Properties: Advances in Caco-2 Cell Monolayer Permeability Modeling. *Curr. Top. Med. Chem.* **2018**, *18*, 2209–2229. [[CrossRef](#)]
34. Broccatelli, F.; Salphati, L.; Plise, E.; Cheong, J.; Gobbi, A.; Lee, M.L.; Aliagas, I. Predicting Passive Permeability of Drug-like Molecules from Chemical Structure: Where Are We? *Mol. Pharm.* **2016**, *13*, 4199–4208. [[CrossRef](#)]
35. Press, B.; Di Grandi, D. Permeability for intestinal absorption: Caco-2 assay and related issues. *Curr. Drug Metab.* **2008**, *9*, 893–900. [[CrossRef](#)]
36. Ertl, P.; Rohdem, B.; Selzer, P. Fast calculation of molecular polar surface area as a sum of fragment-based contributions and its application to the prediction of drug transport properties. *J. Med. Chem.* **2000**, *43*, 3714–3717. [[CrossRef](#)]
37. Zhivkova, Z.D. Studies on drug-human serum albumin binding: The current state of the matter. *Curr. Pharm. Des.* **2015**, *21*, 1817–1830. [[CrossRef](#)] [[PubMed](#)]
38. Colmenarejo, G. In silico prediction of drug-binding strengths to human serum albumin. *Med. Res. Rev.* **2003**, *23*, 275–301. [[CrossRef](#)] [[PubMed](#)]
39. Klein, H.F.; Hamilton, D.J.; de Esch, I.J.P.; Wijtmans, M.; O'Brien, P. Escape from planarity in fragment-based drug discovery: A synthetic strategy analysis of synthetic 3D fragment libraries. *Drug Discov. Today* **2022**, *27*, 2484–2496. [[CrossRef](#)] [[PubMed](#)]
40. Benardout, M.; Le Gresley, A.; ElShaer, A.; Wren, S.P. Application of fSP3 towards Non-Systemic Drug Discovery. 2023; pre-print. [[CrossRef](#)]
41. Wei, W.; Cherukupalli, S.; Jing, L.; Liu, X.; Zhan, P. Fsp3: A new parameter for drug-likeness. *Drug Discov. Today* **2020**, *25*, 1839–1845. [[CrossRef](#)]
42. Ward, S.E.; Beswick, P. What does the aromatic ring number mean for drug design? *Expert Opin. Drug Discov.* **2014**, *9*, 995–1003. [[CrossRef](#)] [[PubMed](#)]
43. Ritchie, T.J.; Macdonald, S.J.; Young, R.J.; Pickett, S.D. The impact of aromatic ring count on compound developability: Further insights by examining carbo- and hetero-aromatic and -aliphatic ring types. *Drug Discov. Today* **2011**, *16*, 164–171. [[CrossRef](#)] [[PubMed](#)]
44. Bajorath, J. Evolution of assay interference concepts in drug discovery. *Expert Opin. Drug Discov.* **2021**, *16*, 719–721. [[CrossRef](#)] [[PubMed](#)]
45. Symeonidis, T.; Chamilos, M.; Hadjipavlou-Litina, D.J.; Kallitsakis, M.; Litinas, K.E. Synthesis of hydroxycoumarins and hydroxybenzo[f]- or [h]coumarins as lipid peroxidation inhibitors. *Bioorg. Med. Chem. Lett.* **2009**, *19*, 1139–1142. [[CrossRef](#)]

46. Li, S.Y.; Wang, X.B.; Xie, S.S.; Jiang, N.; Wang, K.D.; Yao, H.Q.; Sun, H.B.; Kong, L.Y. Multifunctional tacrine-flavonoid hybrids with cholinergic, β -amyloid-reducing, and metal chelating properties for the treatment of Alzheimer's disease. *Eur. J. Med. Chem.* **2013**, *69*, 632–646. [[CrossRef](#)]
47. Daina, A.; Michelin, O.; Zoete, V. SwissADME: A Free Web Tool to Evaluate Pharmacokinetics, Drug-Likeness and Medicinal Chemistry Friendliness of Small Molecules. *Sci. Rep.* **2017**, *7*, 42717. [[CrossRef](#)]

Disclaimer/Publisher's Note: The statements, opinions and data contained in all publications are solely those of the individual author(s) and contributor(s) and not of MDPI and/or the editor(s). MDPI and/or the editor(s) disclaim responsibility for any injury to people or property resulting from any ideas, methods, instructions or products referred to in the content.